A New Communication-less Harmonic-based Protection Architecture for Meshed Microgrids

Siavash Beheshtaein¹, Robert Cuzner², Andrea Benigni³, Mehdi Savaghebi¹, and Josep M. Guerrero¹

Aalborg University, Aalborg, Denmark¹

University of Wisconsin Milwaukee, Milwaukee, USA²

University of South Carolina, Columbia, South Carolina, USA³

{sib,mes,joz}@et.aau.dk, cuzner@uwm.edu, benignia@ces.sc.edu

Abstract— This paper presents a novel communication protection architecture based on utilizing the selected Distributed Generators (DGs) which provide high-frequency harmonics for harmonic-based overcurrent relays to detect and isolate three-phase faults in meshed microgrids. The most prominent features of this structure include limited number of DGs required to inject harmonics, no need for using centralized communication system, and the fault can be detected and located in all conditions such as load disconnection/connection and DG disconnection/connection. The optimum Time Dial Settings (TDSs) of these relays are obtained by solving a coordination problem with Particle Swarm Optimization (PSO) algorithm. Real-time results are produced using OPAL-RT to show the effectiveness of the proposed method for two different locations of faults in a meshed microgrid.

Index Terms— Fault detection, isolation, harmonic injection, Relay coordination, support vector machine (SVM)

I. INTRODUCTION

Protection is considered to be one of the last barriers to viable Microgrid (MG) implementations. MG protection faces several challenges, including topology changes within the MG and Distributed Generator (DG) impacts that result in limitations to reliable fault discrimination, such as blinding of protection, sympathetic tripping, and weak-infeed loop fault [1]. On the other hand, meshed MG is offered as a promising structure for the future MG to bring higher resiliency and reliability by adding redundant paths. In this structure, the concept of upstream and downstream is not valid, so the performance of conventional protective relays must be evaluated once again [1],[2].

Fuses, reclosers, and overcurrent relays have no capability of isolate faults in looped MG with high penetration of DGs, and they require to be reset after any changes in the MG topology (i.e. islanding, isolation of sources, etc.) [3]. The use of distance relays has also low selectivity and high cost of the voltage transformer [4]. Similar to distance relays, directional relays utilize both voltage and current transformers to determine the fault direction, which result in additional cost increases [5]. Although, differential relay addresses the problem of bidirectional power flow, the implementation cost is even higher due to the need for increased complexity within the

protective devices themselves. Besides these conventional approaches, Fault Current Limiter (FCL) [6], and adaptive protection [7] have been presented to address the protection issues. The main disadvantages of these two approaches are high implementation cost and the need for a central monitoring unit, respectively.

This paper presents a novel protection structure based on using a set of High-Frequency (HF) Overcurrent Relays (HFOCRs) and a set of selected DGs, which have the capability of injecting HF harmonic currents. Once the fault happens, each of the selected DGS analyzes its output signals by a Support Vector Machine (SVM) to detect occurrence of the fault. Then, those DGs that recognize fault, inject distinct HF signals and then measure the impedance of connected lines associated with that harmonic within a 40ms time window. If the measured impedance is below the specific value, the DG continue HF harmonic injection, since the fault occurs in connected line associated with another DG, otherwise the DG will stop injecting HF harmonic current. While two distinct HF harmonic currents are injected, the HFOCRs measure the HF current and send the tripping signal the appropriate circuit breaker to isolate the faulty line. In order to achieve fast response of both main and backup relays, a Particle Swarm Optimization (PSO) algorithm is used to find the optimum values of each set of HFOCRs. Finally, different locations of fault are considered to validate the effectiveness of the proposed method. In order to achieve fast response of both main and backup relays, Particle Swarm Optimization (PSO) algorithm is used to find the optimum values of each directional relay parameters. Finally, different locations of fault are considered to validate the effectiveness of the proposed method.

II. PROPOSED METHOD

As shown in Fig.1, the proposed protection method consists of three main parts including fault detection, harmonic injection by DGs as well as measuring HF impedances, and operation of HFOCRs with optimum settings. In the first step, the fault will be detected by feeding a proper set of features to the SVM classifier. Once the fault is recognized by the DG, that DG injects specific HF harmonic and, after waiting 40ms, measure

the HF impedance of the connected lines. The 40ms is minimum

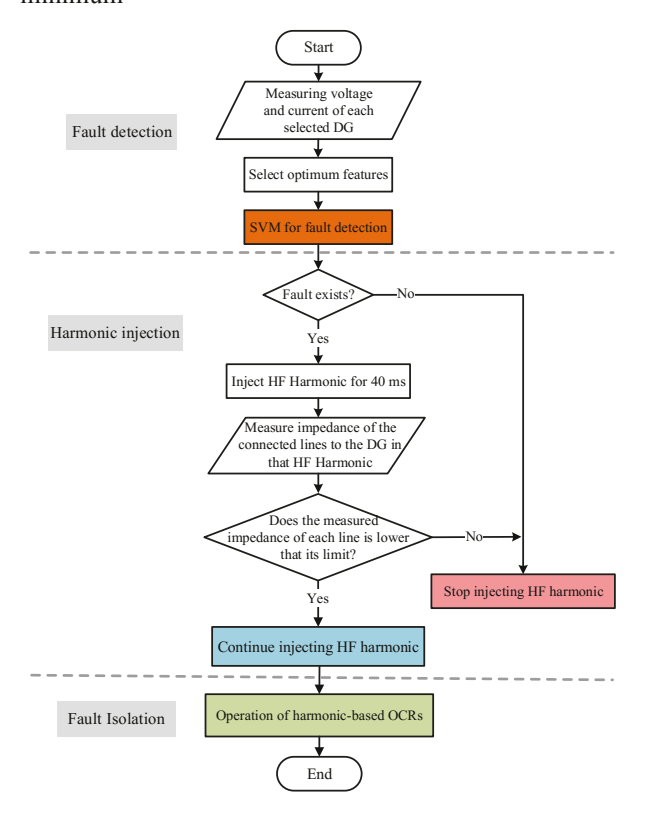


Fig. 1. Scheme of the proposed method.

time requirement for determination of the exact value of impedance by the considered Phased-Locked Loop (PLL). If the measured impedance is below particular value, it means that the fault is located in the connected line. Finally, that DG keep injecting HF harmonic signal to activate corresponding HFOCRs. It must be mentioned that these relays have been coordinated by optimum values for relays settings.

A. Signal Processing Tools for Fault Detection

1) Feature Extraction and Feature Selection

In order to detect the fault, several features including standard deviation, RMS, energy, and Shannon-entropy are extracted from fundamental voltage/current signals. On the other hand, in order to increase the efficiency of SVM classifier in terms of complexity, computation time, and accuracy, the most relative and informative subset of features has to be selected. One of the widely used feature selection algorithms is the sequential forward selection method, which starts with an empty feature set and adds a feature to the set until the accuracy does not change significantly [2]. In the present paper, this method is modified; the algorithm starts with the five best features and the conventional sequential forward selection method is applied to each of these features. The process continues until accuracy of fault classification reaches the desired value.

2) Support Vector Machine

The SVM, which is a powerful binary classifier, adjusts a hyperplane to maximize the margin between two classes.

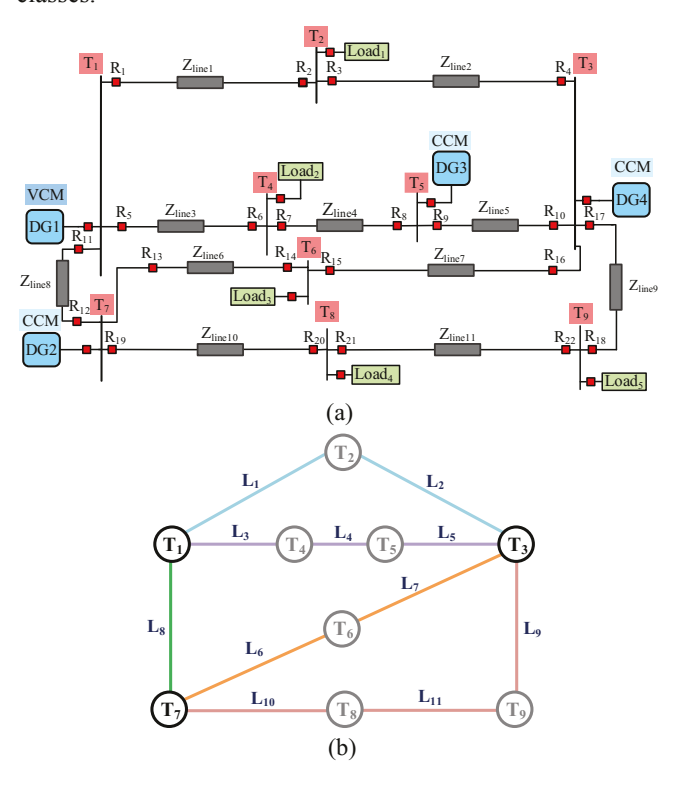


Fig. 2. The meshed microgrid: (a) Scheme of the simulated microgrid, (b) Equivalent graph of the simulated meshed microgrid.

This concept can be formulated as the following primal objective problem:

$$\begin{aligned} &\min j(\omega,\zeta) = \left\{\frac{1}{2} \|\omega\|^2 + C \sum_{i=1}^n \zeta_i\right\} \\ &\text{S.t. } y_i(\omega^T \phi(x_i) + b) \geq 1 - \zeta_i, \zeta_i \geq 0, y_i = \{-1, +1\}^n, \\ &\forall i = 1, 2, \dots, n \end{aligned}$$

where ζ , C, $\varphi(x_i)$ and y_i are the deviation from the margin, penalty factor, a function that maps the testing data vector

 x_i onto high-dimensional feature space, and the corresponding label for each x_i , respectively.

Typically, the primal form of SVM (1) is solved by transforming it to a dual form utilizing Lagrange multiplier method.

$$\min L\left(\alpha\right) = \left\{\frac{1}{2}\sum_{i=1}^{n}\sum_{i=1}^{n}y_{i}y_{j}\alpha_{i}\alpha_{j}K\left(x_{i},x_{j}\right) - \sum_{i=1}^{n}\alpha_{i}\right\}$$
S.t.
$$\sum_{i=1}^{n}\alpha_{i}y_{i} = 0, 0 \leq \alpha_{i} \leq C \ \forall i = 1,2,...,n$$
(2)

where α_i , N, and $K(x_i, x_j) = \Phi(x_i)^T \Phi(x_i)$ are nonnegative Lagrangian multiplier, number of training data, and Kernel function, respectively. Among the different types of Kernel function, the Gaussian Radial Basis Function (RBF) is selected in this paper, defined as follows

$$K(x_i, x_j) = e^{-\gamma ||x_i - x_j||^2}$$
(3)

where γ is the Kernel parameter.

The optimum decision function is achieved by solving this quadratic programming problem using training data with $\alpha_i^* > 0$ called support vectors [3],[4]:

Fig. 3. An illustrative example demonstrating how the proposed harmonic-based relays works.

B. Harmonic injection

1) DGs Selection for Harmonic Injection

Fig. 2 (a) shows a meshed microgrid, where at least one DG has to operate in Voltage Control Mode (VCM) to control voltage and frequency, and other DGs operate in Current Control Mode (CCM) [23]. The corresponding graph of Fig. 2 (a) is shown in Fig. 2 (b). According to Fig. 2 (b), this connection graph has three vertices with a degree higher than two, T₁, T₃, and T₇, as well as the others of degree two.

As described in the proposed method (see Fig. 1), while the fault occurs, the selected DGs detect the fault and inject HF harmonic signals to measure HF impedances of connected-lines from their bus terminals. Existence of bus terminal with more than two connected-lines will cause miscalculation of measured HF impedances. As a result, this bus terminals must be equipped with a DG with capability of harmonic injection. According to this fact, DGs connected to T₁, T₃, and T₇ are selected to inject HF harmonic. From the graph theory viewpoint, the graph is partitioned to two subgraphs, which are defined as the path between two vertices with more than a degree of two.

2) Harmonic injection strategy

When a fault occurs in the meshed MG, two DGs which are closest to the fault inject two distinctive high-frequency harmonics. For example for a fault occurring in Line₃ (see Fig. 3), both DG₁ and DG₄ identify the fault and inject harmonic signal with frequency of 475Hz and 375 Hz for 40 ms, respectively. Because of the location of the fault, the measured HF impedances from DG₁ and DG₄ are both lower than defined limits.

Due to this, HF current flows from DG_1 to the fault. In this case, the R_5 , R_7 , and R_9 measure harmonic current of 475 Hz, and among them, R_5 sends a tripping signal to its corresponding circuit breaker to be opened. Similarly, DG_4 injects HF signal of 375 Hz to activate R_6 , R_8 , and

R₁₀. Finally, R₆ sends a tripping signal to open the corresponding circuit breaker. As can be seen, regardless of MG topology and the number of DGs in MG, only one DG injects HF current and activates its associated HFOCRs. This strategy makes microgrid system behave like a radial grid during the fault. Additionally, the challenges associated with bidirectional power flow, are addressed successfully.

3) Harmonic Selection and Detection

The selection of harmonic components frequency depends on different criteria, such as not interacting with the LCL filter resonant frequency, grid resonant frequency,

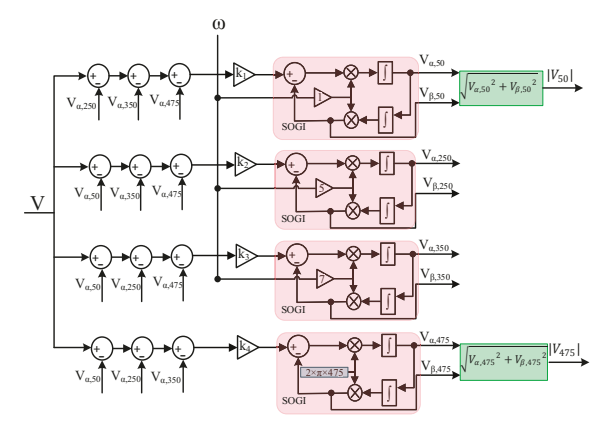


Fig. 4. MSOGI structure for fundamental and harmonic extraction of 475 Hz.

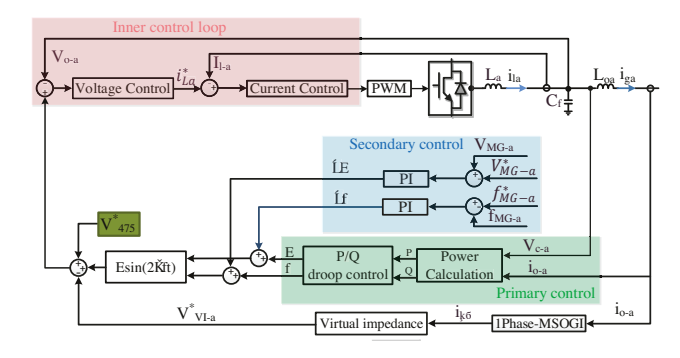


Fig. 5. Scheme of the voltage-control of phase-a of the three-phase four-wire DG with split dc capacitors.

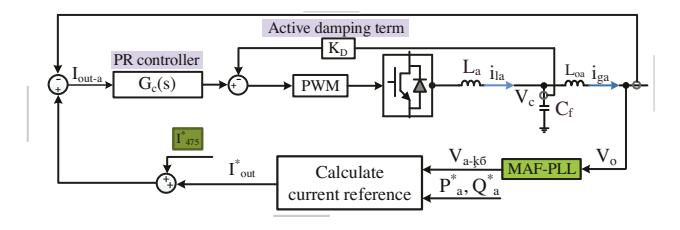


Fig. 6. Scheme of the current-control of phase-a of the three-phase four-wire DG with a split de capacitors regarding harmonic injection.

and fundamental frequency-dependent harmonics [5]. This paper chooses 475 Hz, 375 Hz, and 275 Hz as

appropriate frequencies for the injected signal. In order to detect harmonic and fundamental components, Multiple Order Generalized Integrators PLL (MSOGI-PLL)-based extraction is applied because of its good disturbance rejection capability; fast dynamic response and acceptable computational burden (see Fig. 4 for harmonic extraction of 475 Hz).

4) Control System

MGs may operate in both islanded and gridconnected modes. In the grid-connected mode, voltage and frequency are maintained within the acceptable range by a stiff grid. However, in the absence of a stiff grid, at least one grid forming DG unit is required while the other DGs are grid following units. In this paper, one unit operates in VCM/grid forming (Fig. 5) and others in Current Controlled Mode (CCM)/grid following (Fig. 6). As shown in Figs. 5 and 6, the current and voltage harmonic references of 475 Hz are added to the generated fundamental current and voltage references, respectively. Since DG has to inject votage/current harmonics with 475 Hz independently in each phase, the topology of DG must be three-phase four-wire. Among different topologies of four-wire systems, the three-leg inverter with split dc-link capacitors is popular, where the midpoint of the split dc-link capacitors is connected to a neutral point [6]. As in natural (abc) reference frame Proportional Resonance (PR) controller has better performance than Proportional Integral (PI) one, in the inner loop control, PR controllers are considered for both VCM and CCM, as mentioned bellow

$$G_{V} = k_{PV} + \sum_{h=50,250,350, (s^{2}+2.\omega_{cV}s + (\omega_{h})^{2})} \frac{2.k_{rVh}.\omega_{cV}.s}{(s^{2}+2.\omega_{cV}s + (\omega_{h})^{2})}$$
(6)

$$G_{I} = k_{PI} + \sum_{\substack{h = 50,250,350,\\275,275,475}} \frac{2. k_{rIh}. \omega_{cI}. s}{(s^{2} + 2. \omega_{cI}s + (\omega_{h})^{2})}$$
(7)

where, ω_{cV} and ω_{cI} are the cut-off frequencies for current and voltage loops, respectively. In addition, $k_V(k_I)$ and $k_{rV}(k_{rI})$ are proportional and resonant coefficients of the voltage (current), respectively. In the secondary control level, PI controllers are applied to generate proper control signals to restore both frequency and voltage to their nominal values. As shown in Fig. 6, for CCM-inverter the current reference is generated according to active and reactive powers references. Then, similar to VCM-inverter, the current error passes through PR controller defined as follows [7]:

$$G_{CI} = k_{pII} + \sum_{\substack{h=50,250,350\\275,375,475}} \frac{2. k_{rIIh}. \omega_{cI}. s}{(s^2 + 2. \omega_{cI} s + (\omega_h)^2)}$$
(8)

C. Relay Coordination

1) Coordination formula

The purpose of each protection system is high-speed action of primary protection as well as reliable coordination of backup relay with its primary one. This assumption can be formulated as follows:

Minimize:
$$\sum_{i=1}^{N} t_i(x_{closed-in})$$
 (9)

 $subject\ to: TDS_{min} < TDS < TDS_{max}$

$$t_{bj} - t_{mj} > CTI$$
 & $t_{min} < t < t_{max}$

where, t_i is operation time of primary relay for closed-in fault. The Coordination Time Interval (CTI) is minimum values between operation time of primary and backup relay. For numerical relay CTI as well as TDS_{min} , TDS_{max} and t_{min} is usually considered to be 0.1, 0.015, 1, 0.05. The

Table . Control parameters of the meshed microgrid

Parameters	Symbol	Value
Voltage proportional term of VCM	\mathbf{k}_{pV}	1
Voltage resonant term of VCM ($h=50$)	$\mathbf{k}_{\mathrm{rV50}}$	50
Voltage resonant term of VCM ($h \neq 50$)	$\mathbf{k_{rVh}}$	10
Current proportional term of VCM	$\mathbf{k}_{ exttt{pI}}$	20
Current resonant term of VCM ($h=50$)	$\mathbf{k}_{\mathbf{r}\mathbf{I}}$	1000
Current resonant term of VCM ($h \neq 50$)	$\mathbf{k}_{ ext{iIh}}$	500
Cut-off frequency	ω_{cV}	2
Cut-off frequency	ω_{cI}	2
Current proportional term of CCM	$\mathbf{k}_{\mathtt{p}\Pi}$	300
Current resonant term of CCM ($h=50$)	$K_{r\Pi 50}$	2500
Current resonant term of CCM $(h \neq 50)$	\mathbf{k}_{rm}	2500
Damping factor	K_D	300
Virtual resistance for 50 Hz	R_{v50}	4 Ω
Active power droop term	$\mathbf{k}_{\mathtt{pP}}$	0.0003
Active power droop integral term	$\mathbf{k_{iP}}$	0.0015
Reactive power droop term	\mathbf{k}_{pQ}	0.2
Frequency proportional term	$\mathbf{k_{pf}}$	0.01

Table . Electrical parameters of the meshed microgrid.

Parameters	Symbol	Value
DC voltage	V _{dc}	650 V
Microgrid voltage	$ m V_{microgrid}$	311 V
Microgrid frequency	F	50 Hz
Filter capacitance	C	25 μF
Filter inductance	L	1.8 mH
Output inductance	L_{o}	1.8 mH
Constant active power load	P_{L1}	1500 W
Constant active power load	P_{L3} , P_{L4}	1000 W
Constant resistive load	R_{L2} , R_{L5}	70.53 Ω
	Z_{L1}, Z_{L3}, Z_{L4}	
Line resistance	Z_{L5} , Z_{L6} , Z_{L7}	1+j0.43 Ω
	Z_{L8}, Z_{L10}, Z_{L11}	
Line resistance	Z_{L2} , Z_{L9}	2+j0.86 Ω

operation time of the relay is typically considered to be as current-time characteristics, which is defined as follows:

$$t = \left(\frac{0.14}{\left(\frac{I_{fault}}{I_{pick}}\right)^{0.02} - 1}\right).TDS \tag{10}$$

2) PSO algorithm

In order to find and optimum value of TDSs, a PSO algorithm is used [8]. This algorithm is formulated as follows:

$$\begin{aligned} V_i^{t+1} &= \omega \times V_i^t + C_1 \times rand_1(.) \times (Pbest_i - X_i^t) + \cdots \\ & C_2 \times rand_2(.) \times (Gbest_i - X_i^t) \\ X_i^{t+1} &= X_i^t + V_i^{t+1} \\ i &= 1, 2, 3, \dots, N \end{aligned} \tag{11}$$

Where, C_1 , C_2 are called learning factors and ω is inertia weight.

III. REAL-TIME SIMULATION RESULTS

A meshed MG shown in Fig. 2 (a) with its parameter (see Table I and II) is simulated in OPAL-RT with sampling time 20µs to validate the effectiveness of the proposed method. This is the smallest time-step that the OPAL-RT solver can use in its core computer, where the simulation model is located, and still operate in real-time. In order to have highly efficient fault detection method, various conditions such as different load levels, load switching, DG switching, and different amounts of fault resistance and fault locations are taken into account for training the SVMs (with C and y parameters respectively equal to 4 and 10). Then, modified sequential forward selection algorithm is used to choose the best set of features. According to Table III, where inst. is short form of instantaneous, the selected features for fault detection include energy of phase voltages. It must be noted that each DG injects particular high-frequency harmonic signal for activating only forward/backward harmonicbased relays. For example, in case of Line3, Line4, and Line₅, DG₁ and DG₄ inject voltage harmonics of 475 Hz and 375 Hz to forward relays (R5, R7, and R9) and backward relays (R6, R8, and R10), respectively. Due to this strategy, each set of forward/backward relays behaves like a directional relay without the need of a voltage transformer. It must also be emphasized that optimum parameters of the relays are obtained by solving equations (9) and (10) by PSO algorithm. For example, the optimum values of IP and TDS of relays in Line3, Line4, and Line5 are presented in Table

In order to evaluate the effectiveness of the proposed method, two faults are exerted separately in different locations at 0.5s. In the first scenario, the load₂ and DG₃ are disconnected from islanded microgrid at 0.3 s and 0.4 s, respectively. As can be seen in Fig. 7 (b), the current of DG₄ will be increased and then decreased, respectively. It must be noted that DG₁ and DG₄ operate in VCM and the constant power control mode, respectively. In both cases, the fault detection algorithm does not recognize the disconnection of load₂ and DG₃ as the faulty condition (See Fig. 7 (f)). After these non-fault scenarios, a three-phase fault with R_f =0.2 Ω is applied in Line₄ to examine

the performance of proposed protection system. As shown in Fig. 7 (f), the fault is detected after 0.45ms. Then, according to harmonic injection strategy, DG₁ (see Fig. 7 (a)) injects voltage harmonic of 25 volt at 475 Hz for 40ms to measure impedance of connected line. As it can be seen from Fig. 7 (c), the measured impedance at 475 Hz is below the limit value, which is considered to be 12 Ω . This injected current of 475 Hz activates R₇ after around a 0.1453s and this side of the faulty line will be disconnected. While CB₇ is opened the measured impedance at 475 Hz is increased to reach 12 Ω , then the command for harmonic injection is stopped (see Fig. 7 (c)).

Table . Feature selection for fault detection based on modified sequential forward algorithm.

Selected Features in each step	Class Type Accuracy	
	Normal	ABCG
Energy (I _C)	70 %	55 %
RMS (I _C)	50 %	100 %
Energy (V _C)	0 %	83.33 %
RMS (V _c)	0 %	94.44 %
Inst.(V _c)	0 %	94.44 %
Energy (I _C) & Energy(V _A)	100 %	94.44 %
RMS (I _C) & RMS (V _B)	50 %	94.44 %
Energy(V _C) & Energy(V _B)	50 %	100 %
RMS (V _C) & Inst.(V _B)	0 %	94.44 %
Inst.(V _c) & Inst. (V _B)	40 %	88.89 %
Energy(I _C) & Energy(V _A)& Energy(V _B)	100 %	100 %
RMS (I _C) & RMS (V _B) & Inst. (V _A)	80 %	94.44 %
Energy(V _C)&Energy(V _B)& Energy(V _A)	100 %	100 %
RMS (V _C) & Inst. (V _B) & Inst. (V _A)	100 %	94.44 %
Inst. (Vc) & Inst. (VB) & Inst. (IA)	60 %	88.89 %

Table Optimum values of TDSs and pickup currents for the relays in Line₃, Line₄, and Line₅.

Relay number	I_p	TDS
R ₅	0.2 amp (475 Hz)	0. 0985
\mathbb{R}_7	0.2 amp (475 Hz)	0. 0536
R ₉	0.2 amp (475 Hz)	0. 0179
R ₆	0.2 amp (375 Hz)	0. 0130
R ₈	0.2 amp (375 Hz)	0.0190
R ₁₀	0.2 amp (375 Hz)	0. 0690

Similarly, while DG₄ identifies the occurrence of the fault, the harmonic current with the value of 2.5 A at 375 Hz (see Fig. 7 (e)) is generated to find out if the measured impedance in this frequency is lower than the set value (12 Ω). As can be seen in Fig. 7 (g), the measured impedance at 375 Hz is around 6 Ω , and therefore DG₄

keeps injecting harmonic at 375 Hz. This HF current activates R_8 at 0.5864 s and faulty line will be isolated completely. Finally, the measured impedance at 375 Hz is increased to 12 Ω , and therefore the command signal for harmonic injection of DG_4 is returned to zero.

In the second scenario, a three-phase fault with R_f =0.3 Ω is exerted in line, at 0.5s. While the fault occurs at 0.5

s, DG $_2$ and DG $_4$ identifies the fault at 0.5045 s. Both of them inject HF currents into the meshed microgrid for 40 ms. As shown in Fig. 8 (c), the measured impedance of faulty line at 275 Hz from DG $_2$ bus terminal is around 7 $\Omega.$ It must be noted that this DG works in the constant current control. As this value is lower than set value of the measured

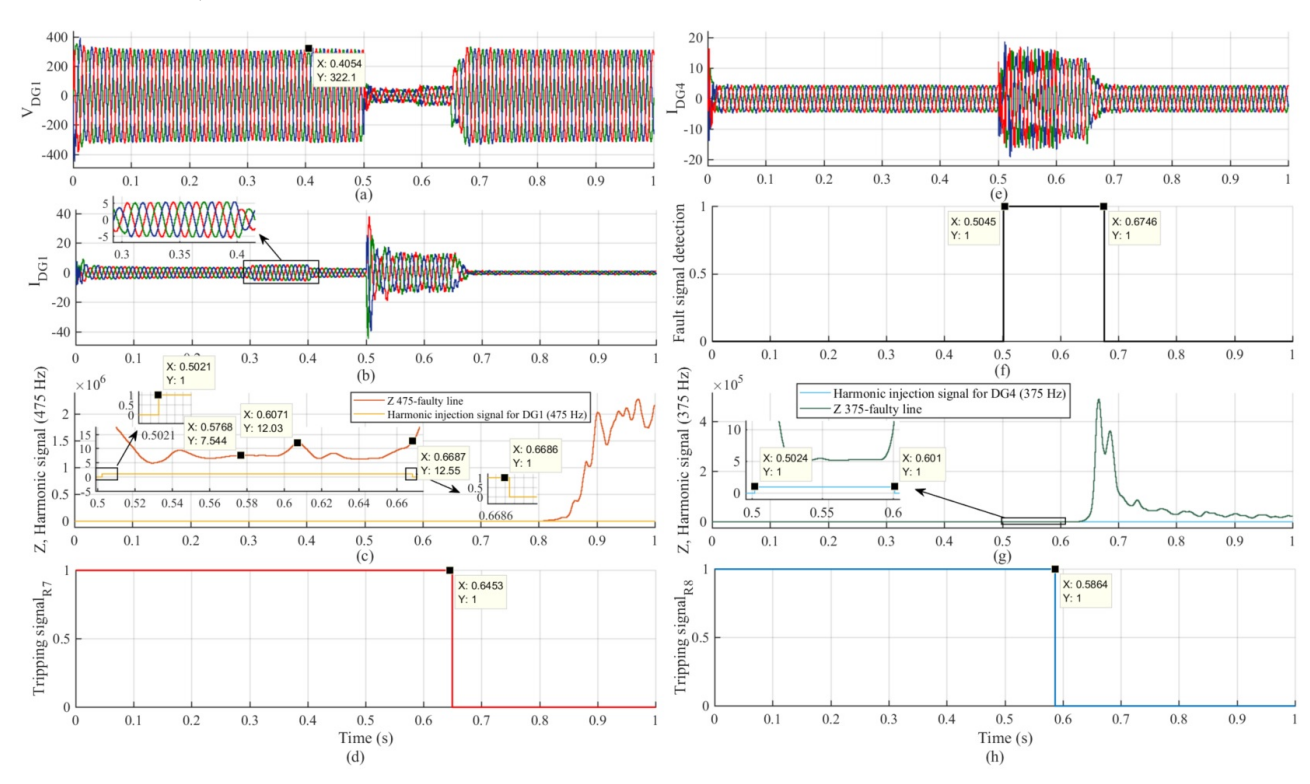
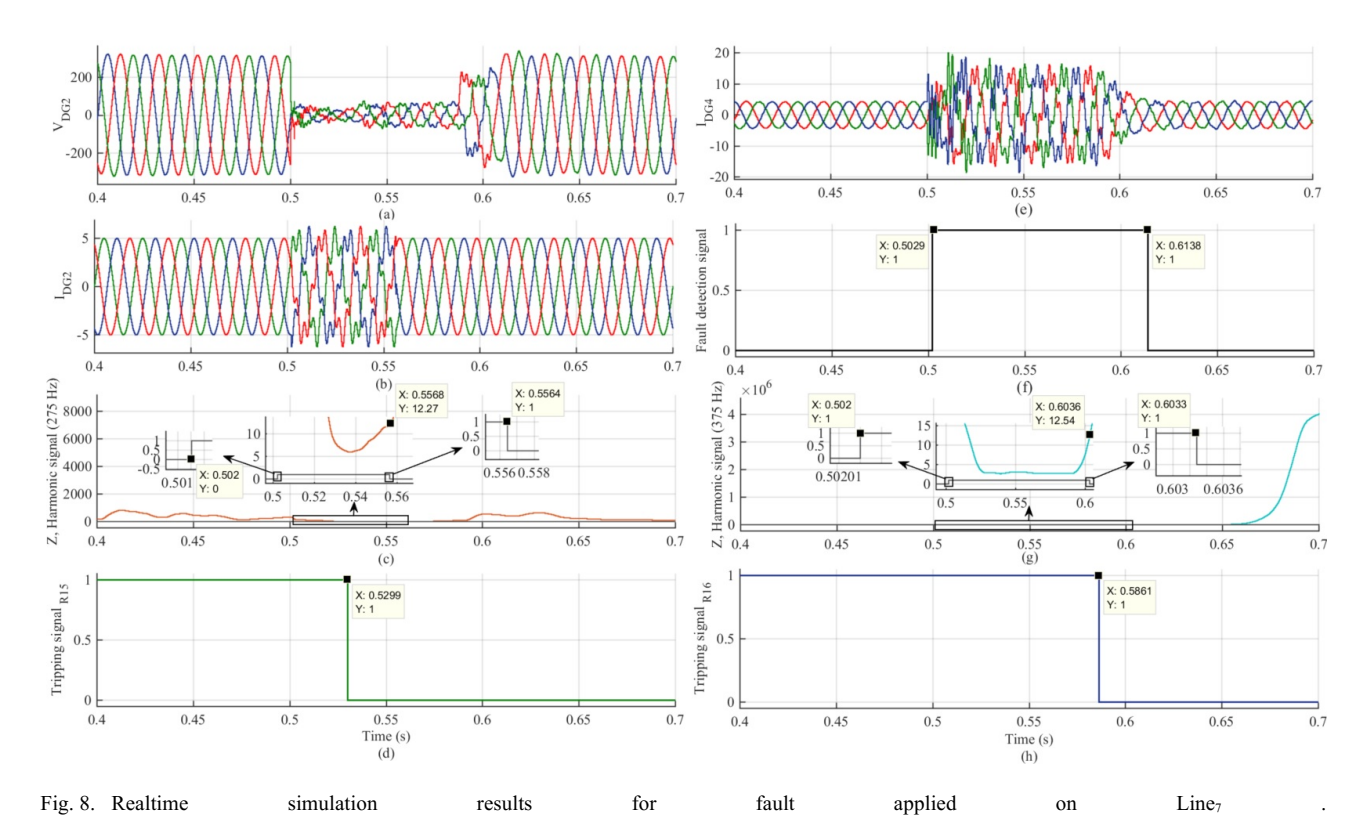


Fig. 7. Realtime simulation results for fault applied on Line₄.



impedance, which is 12 Ω , this DG keep injecting harmonic at 275 Hz. The injected harmonic signal activate the R₁₅ at 0.6453 s (see Fig. 8 (d)). While this side of faulty gets disconnected, the measured impedance in this frequency is increased to exceed the set value. After passing 12 Ω , the DG₂ stop injecting the HF harmonic current (see Fig. 8 (c)). On the other hand, DG₄ measures HF impedances of connected lines at 375 Hz. As it can be seen in Fig. 8 (g), the measured impedance at 375 Hz is around 5 Ω , therefore this DG continues injecting of the HF current. Regarding the optimum value of R₁₆ obtained by PSO algorithm, this relay send the tripping singal to its corresponding circuit breaker to be opened at 0.5864 s. At this time, the faulty line is isolated completely.

IV. CONCLUSION AND FUTURE WORKS

In this paper, a new high-frequency protection structure is proposed to detect and isolate fault by injecting harmonic signals. According to the strategy of harmonic injection, the selected DGs provide HF currents to activate the HFOCR. Thanks to this strategy, different configuration and topology changes of microgrid, which affect the fundamental fault current characteristic, have no adverse effect on the performance of the purposed protection. Therefore, this method does not need to adaptively change time-trip settings to achieve the best possible performance for each topology of the microgrid. Other advantages of this method are no need for communication systems and the HFOCRs only measure HF current for their operation.

The real-time results of two scenarios validate the effectiveness of the proposed method for different situations such as DG and load disconnection/connection in two

different fault locations, and fault impedances. However, this paper has not considered other types of faults. In addition, the meshed microgrid only operates in islanded mode and not grid-connected mode. Accordingly, future works will extend this protection strategy to address and cover those situations.

ACKNOWLEDGMENT

This work was supported in part by the National Science Foundation, grant no. 1439700.

REFERENCES

- [1] S. Beheshtaein, M. Savaghebi, J. C. Vasquez, and J. M. Guerrero, "Protection of AC and DC microgrids: Challenges, solutions and future trends," in *IECON 2015 41st Annual Conference of the IEEE Industrial Electronics Society*, 2015.
- [2] Huseyin Eristi, A. Ucar, and Y. Demir, "Wavelet-based feature extraction and selection for classification of power system disturbances using support vector machines," *Electr. Power Syst. Res.*, vol. 80, pp. 743–752, 2010.
- [3] H. Livani, S. Member, C. Y. Evrenosoglu, and S. Member, "A Machine Learning and Wavelet-Based Fault Location Method for Hybrid Transmission Lines," *IEEE Trans. Smart Grid*, vol. 5, no. 1, pp. 51–59, 2014.
- [4] S. Beheshtaein, M. Savaghebi, J. C. Vasquez, and J. M. Guerrero, "A hybrid algorithm for fault locating in looped microgrids," in ECCE 2016 IEEE Energy Conversion Congress and Exposition, Proceedings, 2016.
- [5] D. D. Reigosa, F. Briz, S. Member, C. B. Charro, P. García, and J. M. Guerrero, "Active Islanding Detection Using High-Frequency Signal Injection," *IEEE Trans. Ind. Appl.*, vol. 48,

- no. 5, pp. 1588–1597, 2012.
- [6] R. Ghosh and G. Narayanan, "Control of Three-Phase , Four-Wire PWM Rectifier," *IEEE trans. Power Electron.*, vol. 23, no. 1, pp. 96–106, 2008.
- [7] J. He and Y. W. Li, "Generalized Closed-Loop Control Schemes with Embedded Virtual Impedances for Voltage Source Converters with LC or LCL Filters," *IEEE Trans. Power Electron.*, vol. 27, no. 4, pp. 1850–1861, 2012.
- [8] S. Beheshtaein, "FAΘPSO based fuzzy controller to enhance LVRT capability of DFIG with dynamic references," in *IEEE International Symposium on Industrial Electronics*, 2014.